International Core Journal of Engineering Volume 7 Issue 11, 2021
ISSN: 2414-1895 DOI: 10.6919/ICJE.202111_7(11).0053

Design, Modeling and Analysis of Four-Coil Inductive Power Transmission System

Shiqi Li*

Chongqing Vocational College of Public Transportation, Chongqing China;

*Corresponding author: 1548027557@qq.com

Abstract

Wireless power transfer (WPT) has been made feasible in recent years due to advances in technology and better implementations of transfer techniques, such as Microwave Power Transfer (MPT). The MPT system works by converting power to microwaves through a microwave generator and then transmitting that power through free space where it is received, and converted back to power at a special device called a rectenna. The applications of MPT are numerous, not only to change the way existing technologies work, but also as theoretical constructs for future constructs. While the benefits are great, there are many limitations and drawbacks of MPT, necessitating the discussion of possible alternative methods for WPT. The transfer of power wirelessly has the potential to completely disrupt and revolutionize existing and future technologies. WPT is an extremely useful technology that has numerous applications and benefits. Mobile phones, laptops and other mobile devices can work normally without plugging in power, and cars can drive on highways that do not use fossil fuels, and wireless power may even solve many of the renewable energy problems we face.

Keywords

Power Transfer; Modeling; Electric cars.

1. Introduction

The transfer of power from source to receiver is a technology [1-4] that has existed for over a century. Since the industrial revolution, with the rapid development of productivity and the rapid progress of modern society, energy has become the focus of attention all over the world. For a long time, fossil energy has been the main resource to support production and life. However, in recent years, due to the increasing demand, the pollution problems caused by fossil fuels and their limited reserves are becoming more and more obvious, and people's demand for new energy is becoming stronger and stronger. As a mature secondary energy, electric energy has attracted more and more attention (as shown in Fig. 1 for main components of a WPT system for EVs). In many applications, electric energy began to gradually replace fossil energy. For example, electrified railway and maglev train gradually replace traditional diesel locomotives, electric vehicles replace traditional diesel locomotives, induction cooker replaces traditional natural gas stove, electric water heater replaces traditional gas water heater, and so on.

ISSN: 2414-1895 DOI: 10.6919/ICJE.202111_7(11).0053

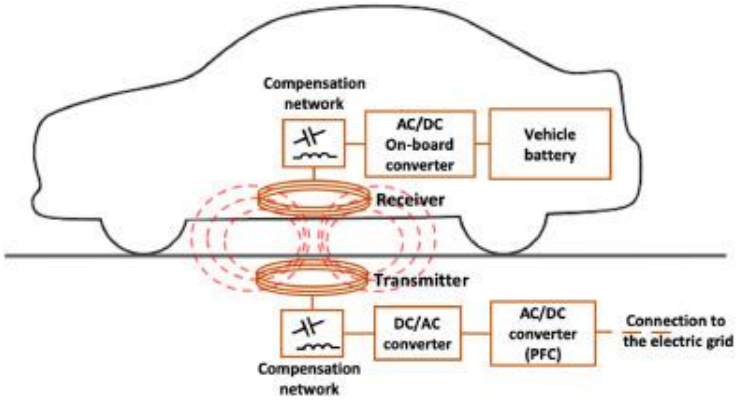

Fig. 1 Illustration of the main components of a WPT system.

Over the past hundred years, numerous scholars have been pursuing their goals tirelessly and put forward a variety of feasible wireless energy transmission schemes. After summing up, it can be considered that wireless power transfer (WPT) technology [5-10] makes use of the distribution and propagation characteristics of electromagnetic field and electromagnetic wave in space, converts electric energy into other forms of intermediate energy at the transmitting end, and then converts it into electric energy after being received by the receiving end, so as to realize direct contact without wire. Radio energy transmission technology is an interdisciplinary frontier technology, which involves many disciplines and fields such as physics, materials science, and biology and control science. It is considered to be a revolutionary application technology.

2. Recent progress and Wireless power transfer Applications

Wireless power transfer via a dielectric loaded multimoded split cavity resonator (SCR) was proposed previously [11], unlike conventional inductive resonant coupling, the scheme enables the control of both the real and imaginary parts of the transfer impedance. It was demonstrated through measurements, analytical models, and extensive full-wave simulation that the inclusion of dielectric resonators (DRs) tuned to the SCR $TE012$ mode significantly enhances the system figure of merit, optimal efficiency, and maximum power transferred to the load. The effect of the DRs is shown to be related to the resonant coupling of the DR $TE01\delta$ and SCR modes, resulting in an electromagnetic induced transparencylike window. An efficiency of 70% is achieved when the transfer distance is 7 cm or half wavelength. Additionally, it was shown that the efficiency is above 40% over a relatively wide bandwidth and a wide range of optimum load impedance. A circuit model was developed that enables the decomposition of the two port network parameters into their modal contributions. Hence, it allows the comparison with conventional inductive resonant coupling systems on the fundamental level.

Coupled resonators enable WPT via the possible electromagnetic coupling between them and their high Q values. The FOM of a WPT system [11] can be expressed as the product κQ. From a circuit theory perspective, coupled resonators can be modeled by a two port network, thus allowing the FOM to be written in terms of circuit parameters as follows:

$$\mathrm{FOM} = \frac{|Z_{21}|}{\sqrt{r_{11}r_{22}-r_{21}^2}} = \sqrt{\frac{r_{21}^2/r_{11}r_{22}+x_{21}^2/r_{11}r_{22}}{1-r_{21}^2/r_{11}r_{22}}} \quad (1)$$

where $Zmn=rmn+jxmn$ is the (m,n) element of the $\mathbf{Z}$ matrix. The expression of FOM in (1) is an extended κQ expression that is valid for an arbitrary two port network. Indeed, given a two port network, its maximum efficiency ηmax is fully determined via FOM. As was previously shown, if FOM is represented by the tangent of an angle 2θ (i.e., FOM≙tan2θ), ηmax is precisely tan2θ. Equation (1) reveals that the FOM depends on the relative magnitudes of the transfer components $r21$ and $x21$ with respect to the product of self-resistor values $r11$ and $r22$. Accordingly, (1) can be conveniently rewritten as:

ISSN: 2414-1895 DOI: 10.6919/ICJE.202111_7(11).0053

$$\text{FOM} = \sqrt{\frac{r_n^2 + x_n^2}{1 - r_n^2}} \quad (2)$$

Therefore, the FOM can be enhanced by increasing rn and/or xn.

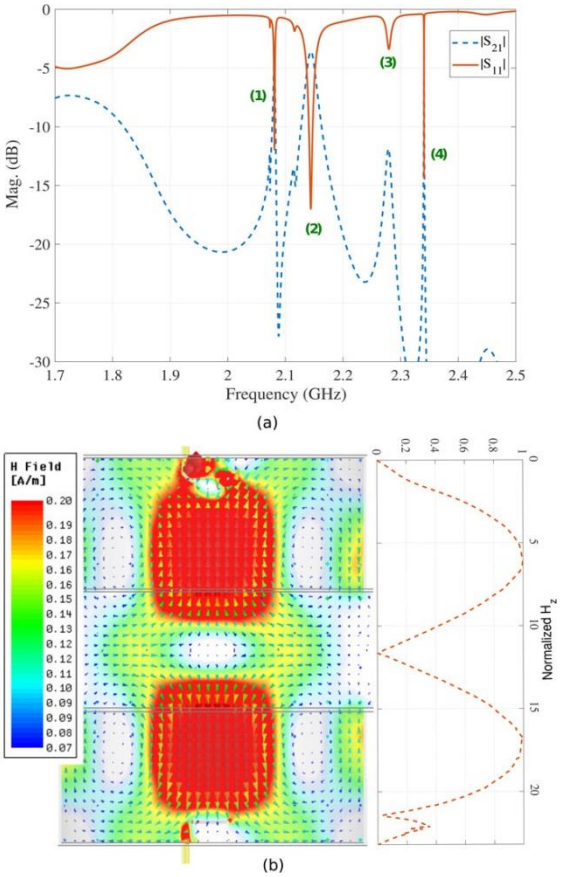

Fig. 2 (a) Simulated S parameters of the SCR when displaced 7 cm apart [11]. (1)–(4) denote the positions of the resonant modes. (1): $TM111$ at f=2.081GHz, (2): $HEM111$ at f=2.145GHz, (3): $TM112$ at f=2.28GHz, and (4): $TE012$ at f=2.34GHz. (b) Simulated magnetic field along the axial axis Hz of the $TE012$ mode.

Figure 2(a) presents the magnitude of the simulated $S11$ and $S21$ parameters. The dips in $S11$ represent the excited modes as highlighted in the figure. Inspecting the field profile of the second mode reveals that it is a hybird mode. The fourth mode is a $TE012$ mode with a frequency $fTE012$=2.34GHzf. This mode has a very high Q; in fact, the eigenmode solution redicts its Q∼10000.

In the axial direction, the fields have two nulls [hence the mode is described by two half wavelengths in the axial direction, Fig. 2(b)]. When d=7cm, $f$cut=2.143GHz. Although fTE012>$f$cut, the fields of the $TE012$ do not propagate through the radial waveguide since its field profile does not match the waveguide $TE10$ mode profile. However, if the flange is excessively short, the resonant modes will have lower Q values due to the added radiative losses. To be more specific, $TE20$ is the relevant waveguide mode, which has a cut-off frequency of $fcut$=c/d≈4.3GHz.

Kim et al. [12] introduced a method (as shown in Fig. 3) for adjusting the effective permeability of the ferrite blocks in the standard model, to tune the self-inductance of the coils as well as the coupling coefficient. To guarantee the given values of the self-inductance of the coil and coupling coefficient matched those in the standard, they slightly modified the air-gap between the ferrite tiles in a specific region. Based on this method, it was possible to successfully tune the self-inductance of the transmitting coil and receiving coil as well as the coupling coefficient.

ISSN: 2414-1895 DOI: 10.6919/ICJE.202111_7(11).0053

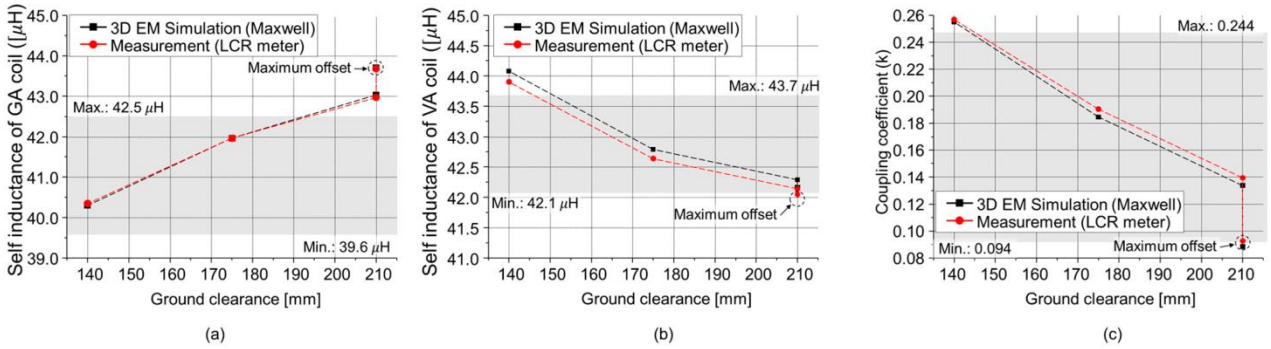

Fig. 3 Measured value and expected value [12] of the self-inductance of the GA, the VA coil and the coupling coefficient. Both of the lGA1 and lGA2 are set as 1 mm. (a) Self-inductance of GA coil; (b) Self-inductance of VA coil; (c) Coupling coefficient (k) between GA coil and VA coil.

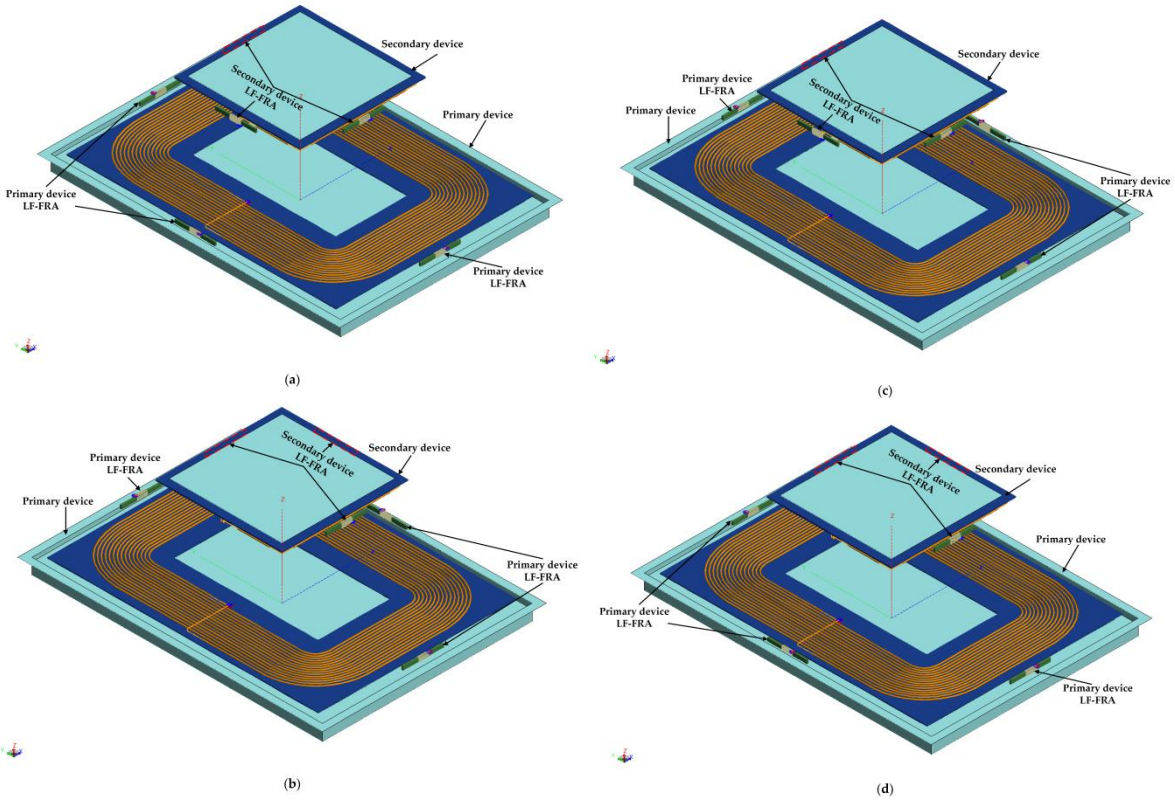

Fig. 4 The geometrical structure [13]: (a) the LF-FRA located on both the primary device's and the secondary device's −x-direction, (b) the LF-FRA located on both the primary device's and the secondary device's x-direction, (c) the LF-FRA located on the primary device's x-direction and the secondary device's −x-direction, and (d) the LF-FRA located on the primary device's −x-direction and the secondary device's x-direction.

The simulated and measured self-inductance values of the GA coil were shown in Fig. 3, the VA coil and the coupling coefficient, including all clearances, as well as the maximum misalign condition (Δx= 75 mm, Δy= 100 mm). Based on the simulated results, the lGA1 and lGA2 were set as 1 mm and 1 mm, respectively. For the measurement, a TH2827C LCR meter was used at 85 kHz. The errors between simulation and measurement were lower than 4.5%. The highest out of range given in the SAE J2954 standard for the self-inductance of the GA, VA and coupling coefficient were 0.5%, 2.8%, and 5.6%, respectively.

Lee et al. [13] designed and modeled an optimized arrangement of a LF-FRA for the fine positioning of an EV MF-WPT in accordance with IEC 61980 and SAE J2954 standards. The geometric dimensions of the LF-FRA for fine positioning of an EV MF-WPT confirmed the pre-condition that it might have 70 turns on a ferrite rod width of 90 mm, length of 10 mm, and thickness of 2.5 mm.

ISSN: 2414-1895 DOI: 10.6919/ICJE.202111_7(11).0053

Third, since the LF-FRA had to be mounted and arranged on the primary and secondary devices, the size needed to be optimized. Through modeling and simulation, we optimized the LF-FRA for EV MF-WPT fine positioning.

Two conditions were considered regarding the arrangement of LF-FRAs in the primary device and the secondary device. The first condition was the near field B-field distance of the LF-FRA. In other words, the near field B-field distance used for fine positioning was the distance from the geometrical center of the primary device to the B-field formed by the x-direction and the secondary device in the B-field formed by the −x-direction. The second condition was as follows: Even if the B-field of the LF-FRA of the primary device overlapped with the B-field of the secondary device, the LF-FRA, acting as a receiver, should have been able to accurately recognize the distance. Therefore, the optimal arrangement of the LF-FRA for the fine positioning of an EV MF-WPT that satisfied these two conditions was to arrange the LF-FRA in the −x- and ±y-direction for the primary device and the x- and ±y-direction for the secondary device.

3. Modeling and Analysis

Compared to 2-coil MCR-WPT systems, 4-coil systems have also received worldwide attention since this coil structure can greatly improve the performance of WPT system [14]. Figure 5 depicts the basic structure of 4-coil WPT system. In general, both the driven and load loop are single copper loops and Tx and Rx ports are multi-turn coils. In some cases, two coils in the middle will rely on self-resonance. The copper wire has its own resonance frequency because of the self-inductance of the coil and the stray capacitances between the spiral wires. However, in most instances, additional capacitances are welded to eliminate the imaginary part and used to tune the resonance frequency. In addition, it can reduce the environment impact on the system since the parasitic parameters are sensitive to the surroundings, such as the humidity, temperature and even the human activity.

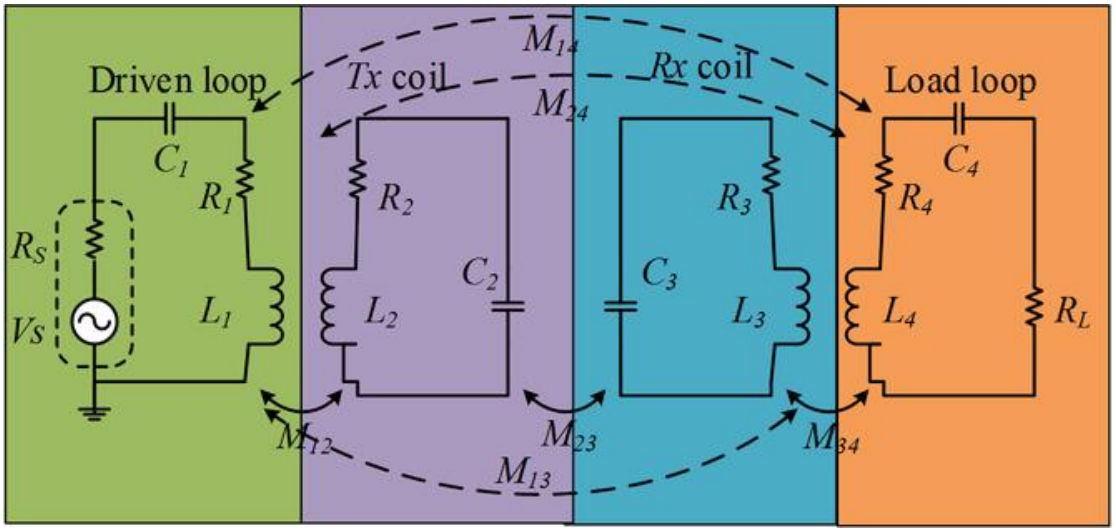

Fig. 5 Basic structure of 4-coil WPT system [14].

In general, for the sake of simplicity, the cross-coupling terms (M13, M12, and M14) are ignored in the 4-coil WPT due to the weak coupling. This is because the coupling coefficient decreases sharply when the distance between the coils increases. The real-power energy efficiency is proportional to the square of the magnetic coupling coefficient, implying that the efficiency drops rapidly with transmission distance. Essentially, the analysis of 4-coil WPT system is similar to that of 2-coil system.

ISSN: 2414-1895 DOI: 10.6919/ICJE.202111_7(11).0053

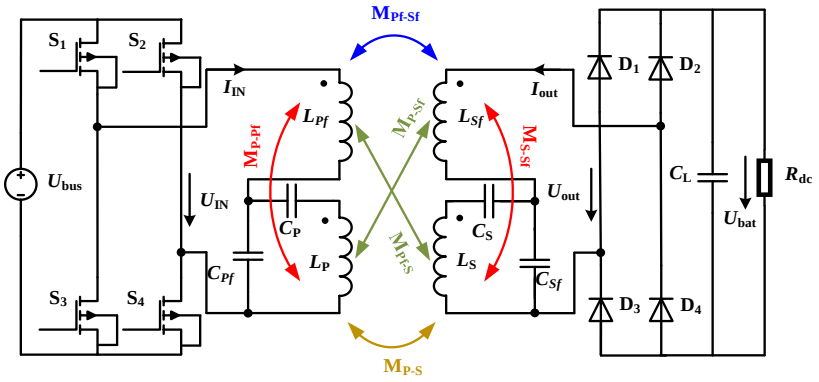

Fig. 6 The topology four coil IPT system as applied in this study.

The circuit topology of the inductive radio energy transmission system is shown in Fig. 6 based on the four coil structure proposed in this study. UBUS is a DC input power supply, which is usually provided by municipal power through rectification, or by DC power supply such as battery.

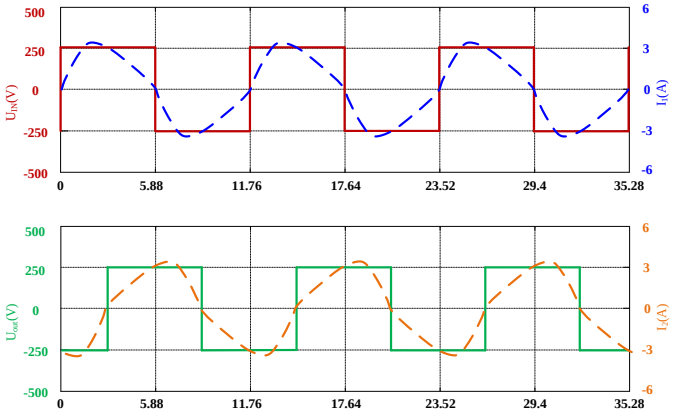

Fig. 7 The input and output current and voltage waveforms as obtained by modeling with Simulink.

It can be seen (as in Fig. 7) that the phases of voltage and current are almost the same at the input and output of the system, and the phase of current is slightly ahead of the voltage, which not only effectively limits the reactive power in the resonant circuit and reduces the power loss, but also helps to realize the soft switching of inverter switch and greatly reduce the switching loss.

4. Conclusion

With the large-scale use of electric energy in the whole society, some weaknesses and limitations of the traditional power supply mode of cable transmission are gradually highlighted. Recent progress and application of wireless power transmission were studied, 2-coil WPT systems with that of 4-coil systems was compared, finally, the modeling and analysis for four coil system was investigated. In the process of power transmission, cable power supply will inevitably produce transmission loss and heating due to the impedance of conductor. At the same time, line aging, tip discharge and other factors are also easy to lead to electric sparks, which greatly reduces the reliability and safety of equipment power supply and shortens the service life of equipment. On the one hand, in some special dangerous operation occasions such as mines and seabed, these shortcomings of the traditional cable power supply mode are often fatal, which is very easy to cause short-circuit leakage, fire, explosion and equipment damage, resulting in great potential safety hazards and economic losses. On the other hand, the power supply of a large number of electrical appliances in life is bound to lead to the intersection of a variety of power lines, which will bring great inconvenience to people's life. In order to get rid of the constraints of energy lines, many engineers and researchers have invested in the research of wireless transmission of electric energy.

ISSN: 2414-1895 DOI: 10.6919/ICJE.202111_7(11).0053

References

[1] Bayguzina, E. and B. Clerckx, Asymmetric Modulation Design for Wireless Information and Power Transfer With Nonlinear Energy Harvesting. Ieee Transactions on Wireless Communications, 2019. 18(12): p. 5529-5541.

[2] Gu, H., et al., Resource allocation for wireless information and power transfer based on WBAN. Physical Communication, 2019. 37.

[3] Hayajneh, M. and T.A. Gulliver, Wireless information and power transfer with optimal transmit antenna selection. Iet Communications, 2019. 13(19): p. 3217-3221.

[4] Liao, K., et al., Distributed Beamforming Design for Nonregenerative Two-Way Relay Networks with Simultaneous Wireless Information and Power Transfer. Wireless Communications & Mobile Computing, 2019. 2019.

[5] Abou Houran, M., X. Yang, and W. Chen, Free Angular-Positioning Wireless Power Transfer Using a Spherical Joint. Energies, 2018. 11(12).

[6] Altawaim, M.N., et al., Outage Performance Analysis for Device-to-Device Communication Underlying Small Cell Networks with Wireless Power Transfer. Mobile Networks & Applications, 2018. 23(6): p. 1597-1606.

[7] Gao, X. and M. Deng, Operator-based robust nonlinear control of an uncertain wireless power transfer system using sliding mode technology. Transactions of the Institute of Measurement and Control, 2018. 40(16): p. 4397-4406.

[8] Hussein, R., et al., A New Design for Compact Size Wireless Power Transfer Applications Using Spiral Defected Ground Structures. Radioengineering, 2018. 27(4): p. 1032-1037.

[9] Mizojiri, S. and K. Shimamura, Wireless Power Transfer via Subterahertz-Wave. Applied Sciences-Basel, 2018. 8(12).

[10] Zhao, J., et al., Analysis and experiments on transmission characteristics of LCCL mobile wireless power transfer system. Ieice Electronics Express, 2018. 15(23).

[11] Elnaggar, S.Y., C. Saha, and Y.M. Antar, Wireless power transfer via dielectric loaded multi-moded split cavity resonator. Journal of Applied Physics, 2019. 126(24): p. 244902.

[12] Kim, D., et al., Analysis and Introduction of Effective Permeability with Additional Air-Gaps on Wireless Power Transfer Coils for Electric Vehicle Based on SAE J2954 Recommended Practice. Energies, 2019. 12(24): p. 4797.

[13] Seong, J.Y. and S.-S. Lee, Optimization of the Alignment Method for an Electric Vehicle Magnetic Field Wireless Power Transfer System Using a Low-Frequency Ferrite Rod Antenna. Energies, 2019. 12(24): p. 4689.

[14] Rong, C., et al., A critical review of metamaterial in wireless power transfer system. IET Power Electronics, 2021. 14(9): p. 1541-1559.